RSC Advances

PAPER

View Article Online
View Journal | View Issue



Cite this: *RSC Adv.*, 2024, **14**, 30037

# Synthesis and fluorescence properties of europium complex functionalized fiberglass paper†

Qiuping Li, *[a] Qianqian Wen,[a] Zian Fang,[a] Yidi Wang,[a] Hongxia Ouyang,*[a] Qi Wang[a] and Meng Wei[b]

Received 16th July 2024
Accepted 16th September 2024

DOI: 10.1039/d4ra05143b

rsc.li/rsc-advances

The development of novel rare earth fluorescent materials and the exploration of their applications have consistently been focal points of research in the fields of materials science and chemistry. In this work, a novel rare earth composite material with good photo-fluorescence properties and self-supporting has been prepared *via* a simple ultrasonic solvent reaction method. Initially, the Phen moieties is immobilized onto the surface of a self-supporting fiberglass paper using ICPTES, followed by the coordination of $Eu(TTA)_3$ moieties with Phen moieties through a convenient ultrasonic solvent reaction. The resulting GF–Phen–$Eu(TTA)_3$ has been characterized using FTIR, UV-Vis DRS, fluorescence measurements, and so on. The results indicate that the composite material exhibits strong fluorescent emission and presents a vivid red color under ultraviolet light. Further research has shown that the fluorescence of GF–Phen–$Eu(TTA)_3$ strips demonstrated a pronounced quenching effect in response to some transition metal ions (1 mM). Hence, the rare earth composite materials presented here can be utilized not only for the production of optical materials, but also for the development of fluorescence sensing strips.



## 1. Introduction

The fluorescence mechanism of rare earth compounds closely resembles atomic emission.[1–3] These compounds exhibit many advantages in fluorescence, including narrow emission bandwidths, long fluorescence lifetimes, and a wide range of colors. Due to their unique luminescent properties, rare earth compound-based luminescent materials have found extensive applications in fields such as luminescent devices,[4–7] chemical sensing,[8–10] biological imaging,[11–13] commodity anti-counterfeiting[14–16] over the past few decades. However, due to the parity forbidden of f → f transition, the direct absorption intensity of rare earth ions is weak, which leads to the application bottleneck associated with the low fluorescence quantum efficiency of many rare earth compounds.[17,18] To address this issue, the incorporation of specific organic ligands for coordinating with rare earth ions represents an efficacious strategy.[19–21] The presence of these ligands can enhance the light absorption coefficient of rare earth compounds in the ultraviolet range, thereby effectively exciting the rare earth ions through a non-radiative energy transfer process and significantly boosting their fluorescence performance. The phenomenon is commonly referred to as the "antenna effect". The ligands commonly employed for sensitizing the luminescence of rare earth ions include derivatives of carboxylic acids,[22–24] β-diketones,[25–27] N-heterocyclic compounds,[28–30] *etc.* The incorporation of these organic ligands not only significantly enhances the fluorescence quantum efficiency, fluorescence emission intensity, and prolongs the fluorescence lifetime but also facilitates the covalent assembly of rare earth complexes onto diverse matrix materials through ligand modification, thereby achieving the construction of multi-component luminescent materials based on rare earth elements.

In recent decades, there has been a significant surge in attention towards this multi-component composite, which is based on the covalent assembly of rare earth complexes.[31–36] The commonly employed matrices for fabricating rare earth multi-component hybrid materials encompass silicon oxide,[37–39] carbon,[40–42] metal oxide,[43–45] polymer,[46–48] and zeolite[49–51] materials. The incorporation of these matrices significantly enhances the stability of rare earth complexes and broadens the application fields of rare earth-based luminescent materials. However, with the exception of polymer-based rare earth multi-component hybrid materials that can be directly shaped, most other types of rare earth multi-component hybrid materials exist in powdered form and cannot undergo direct processing for molding. Therefore, researchers have redirected their focus towards the development of rare earth multi-component hybrid materials based on substrates possessing inherent self-supporting properties such as polymer matrix,[52] glass,[53] fiber,[54] *etc.* For instance, the successful integration of the Europium complex onto ITO Glass by Santos *et al.*[55] resulted in

[a]*FuZhou AI Drug Innovation Center, School of Pharmacy, Fuzhou Medical College of Nanchang University, Fuzhou 344000, China. E-mail: liqiuping@yeah.net; hongxiaoy83@qq.com*

[b]*Jiangxi Yatai Technology Co., Ltd, Yichun 336100, China*

† Electronic supplementary information (ESI) available. See DOI: https://doi.org/10.1039/d4ra05143b

the fabrication of remarkably efficient Organic Light-Emitting Diodes (OLEDs). Shang *et al.*[56] successfully achieved the grafting of europium complexes onto carbon fiber, resulting in the development of a composite material exhibiting strong red fluorescence. Tong *et al.*[57] fabricated a lanthanide Metal–Organic Frameworks functionalized carbon cloth by *in situ* growth method, followed by modification of poly vinyl terephthalic acid through *in situ* polymerization, which resulted in the production of a novel fluorescent composite thin film with exceptional sensitivity towards $UO_2^{2+}$ ions. Currently, the fabrication of rare earth fluorescent composites using self-supporting matrices and their subsequent applications in sensing present a significant challenge.

The glass fiber paper is an environmentally friendly, highly stable, cost-effective, and easily modifiable material that serves as a well self-supporting matrix for fabricating composites.[58,59] Herein, a very simple strategy was proposed to prepare the highly photo-fluorescent rare earth composite by directly surface-modifying glass fiber filter paper. We successfully immobilized a europium complex onto the surface of a glass fiber filter paper using a molecular bridge, resulting in the formation of a composite luminescent material. Finally, the resulting material has been thoroughly investigated in terms of their photophysical properties and their potential application for metal ion sensing.

## 2. Experimental details

### 2.1 Materials and methods

The 1,10-phenanthrolin-5-amine (Phen-$NH_2$, 97%), isocyanatopropyltriethoxysilane (ICPTES, 95%), 2-thenoyltrifluoroacetone (TTA, 98%) and $EuCl_3 \cdot 6H_2O$ (99.99% metals basis) were purchased from Shanghai Aladdin Biochemical Technology Co., Ltd. The glass fiber (GF) filter was purchased from Weifang Kaisheng Electronic Technology Co., Ltd. All other reagents and solvents were obtained from Sinopharm Chemical Reagent Co., Ltd. The Fourier transform infrared spectroscopy (FTIR) were determined Agilent Cary 630. The fluorescence excitation and emission data were tested with SHIMADZU RF-6000 fluorescence spectrophotometer. NMR spectra were recorded on AVANCE NEO 400MHZ. Elemental analysis were tested with Elementar UNICUBE. The ultraviolet-visible diffuse reflection spectrum (UV-Vis DRS) were recorded by Shimadzu UV-3600Plus spectrophotometer. The powder X-ray diffraction patterns (XRD) were acquired on Rigaku SmartLab SE equipped with Cu anode. The fluorescence lifetime was measured on an Edinburgh Instruments FLS 920 fluorescence spectrometer.

### 2.2 Synthesis of europium complex

The lanthanide complexes were synthesized by typical methods. For $Eu(TTA)_3 \cdot 2H_2O$, typically: At room temperature, 6 mmol TTA was dissolved in ethanol, followed by 3 mL 1 mol per L NaOH aqueous solution for deprotonation; And then an ethanol solution containing 2 mmol $EuCl_3 \cdot 6H_2O$ was slowly introduced into the solution. The resulting mixture was stirred for 30 min until it is slowly transformed into the $Eu(TTA)_3 \cdot 2H_2O$ solution. The solution was not further processed and was directly reserved for further use. For elemental analysis and $^1H$ NMR spectroscopy, the solution was initially concentrated to induce the precipitation of $Eu(TTA)_3 \cdot 2H_2O$. The resulting precipitate was subsequently washed with water and petroleum ether, dried, yielding a crude product that was characterized as $Eu(TTA)_3 \cdot 2H_2O$. $^1H$ NMR ($CDCl_3$, 400 MHz, $\delta$ ppm): 7.07 (s, 3H, H of thiophene moiety), 6.51 (s, 3H, H of moiety), 6.07 (s, 3H, H of moiety), 0.88 (s, 3H, H of β-diketonate). Elemental analysis was performed for C, H, S, atoms. Calc. for $EuC_{24}H_{16}F_9O_8S_3$: C, 33.85; H, 1.89; S, 11.30. Found: C, 33.43; H, 2.34; S, 11.32.

### 2.3 Synthesis of europium complex functionalized glass fiber

First, the cut glass fiber was soaked in 25% NaOH solution and activated for about 30 min, then washed with deionized water and dried at 60 °C, denoted GF. Subsequently, the as-prepared GF was immersed in an ethanol solution containing 1 mmol Phen-$NH_2$ and 7 mmol ICPTES. The reaction system was then transferred to an ultrasonic cleaning machine (40 kHz, 50 W) for ultrasonic treatment for 60 min. After treatment, the glass fiber was took out and washed with anhydrous ethanol, and dried at 60 °C to obtain the Phen-loaded glass fiber, which is referred to as GF–Phen. The GF–Phen was immersed in the as-prepared $Eu(TTA)_3 \cdot 2H_2O$ solution and treated in the ultrasonic cleaning machine again for 60 min. Finally, the europium complex functionalized glass fiber was took out and washed with anhydrous ethanol, and dried at 60 °C to obtain the GF–Phen–$Eu(TTA)_3$ (Scheme 1).

### 2.4 Sensing experiments

The GF–Phen–$Eu(TTA)_3$ was cut into strips and immersed in a series of solutions containing different metal ions for 10 min under ultrasonic treatment. Subsequently, the resulting strip

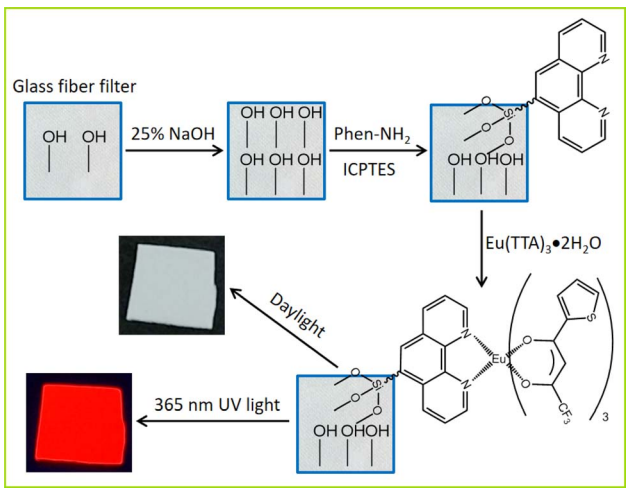


Scheme 1 Synthesis strategy of the europium complex functionalized glass fiber and the photos of the resultant product under daylight and 365 nm UV light.

was extracted and dried prior to conducting fluorescence measurements. All fluorescence measurements were conducted under the same circumstances.

## 3. Results and discussion

The main composition of glass fiber and the other glass is essentially identical, consisting primarily of a mixture of various silicate compounds. Upon activation, the surface of glass fiber becomes enriched with numerous active silicon hydroxyl groups (Si–OH), thereby endowing it with exceptional potential for surface modification and rendering it highly suitable as a matrix material for preparing composite materials. On the other hand, the bridge-linking method is widely recognized as the primary approach for fabricating hybrid materials with covalent bonds, and it has been extensively employed in the synthesis of rare earth composite luminescent materials. Based on these findings, a self-supporting glass fiber filter paper was chosen as the substrate. Its surface was activated with NaOH aqueous solution and subsequently modified with Phen-$NH_2$ and ICPTES in combination to establish a molecular bridge, the obtained materials are marked as GF–Phen. The superior chelating properties of the Phen moiety enable GF–Phen to effectively adsorb unoccupied rare earth complexes on its surface. Ultimately, the rare earth europium complex was immobilized onto the surface of glass fiber through the immersion of GF–Phen in $Eu(TTA)_3 \cdot 2H_2O$ solution followed by ultrasonic treatment, resulting an innovative composite luminescent material (GF–Phen–$Eu(TTA)_3$). The synthesis strategy is shown in Fig. 1. As illustrated, the obtained GF–Phen–$Eu(TTA)_3$ exhibits negligible coloration under daylight; however, it manifests a vivid red color upon irradiation with 365 nm UV light. This transformation can be attributed to the characteristic emission of the europium complex when excited by UV light. It can also be regarded as evidence of the successful immobilization of rare earth complexes onto glass fiber filter paper. At the same time, in order to investigate the impact of surface modification on the microstructure of glass fiber paper, the XRD tests on the glass fiber paper before and after modification were conducted (Fig. S1, ESI†). The results indicate that the surface complexation did not alter the microstructure of the glass fiber paper. Whether before or after modification, the material exhibits a broad peak centered around approximately 25°, indicative of the characteristic diffraction pattern of the amorphous silicon framework material. Furthermore, there are no discernible crystalline regions in the XRD patterns, suggesting that the europium complex introduced during material modification should be at a mesoscale level. Therefore, no relevant crystallographic data appeared in the XRD pattern (Fig. S1, ESI†).

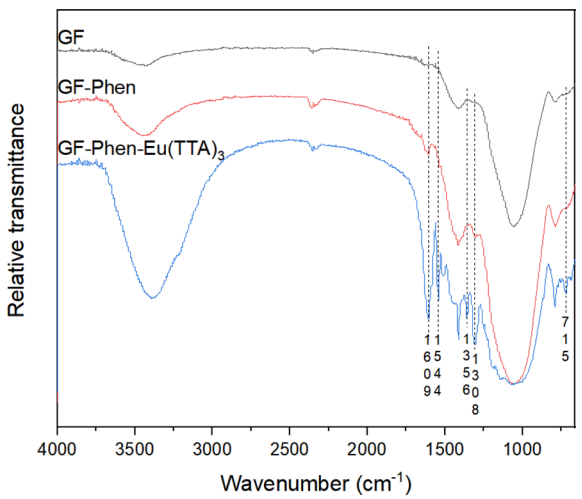


Fig. 1 FTIR spectra of GF, GF–Phen and GF–Phen–$Eu(TTA)_3$.

To further investigate the assembly of europium complexes on the surface of glass fiber, the Fourier transform infrared spectroscopy (FTIR) was employed to characterize the relevant materials. As shown in Fig. 1, the spectrum of GF is characterized by a simple profile and exhibits typical features of silicate infrared spectra; it shows a prominent absorption at 1060 $cm^{-1}$, which derives from the asymmetric stretching vibration of Si–O–Si moieties and consistents with the spectra of GF–Phen and GF–Phen–$Eu(TTA)_3$. The spectrum of GF–Phen closely resembles that of GF, with a more pronounced absorption peak at 1609 $cm^{-1}$, attributed to the stretching vibration of C=O and bending vibration of N–H in amide group. For the GF–Phen–$Eu(TTA)_3$, the peak observed around 1609 $cm^{-1}$ exhibits a notable increase in intensity. This augmentation is primarily ascribed to the stretching vibration of C=O in β-diketone moieties, which shifts to lower wavenumber after coordinating with europium(III) ions. The peak at 1544 $cm^{-1}$ of GF–Phen–$Eu(TTA)_3$ also arises from the downward shift stretching vibration of C=C within the ring-shaped β-diketone coordination structure. Furthermore, the peaks observed at 1308 $cm^{-1}$ and 1356 $cm^{-1}$ are indicative of the symmetric and asymmetric stretching vibrations of the $CF_3$ group, while the peak at 715 $cm^{-1}$ can be attributed to the stretching vibrations of the C–S bond. The presence of these absorption peaks in spectrum of GF–Phen–$Eu(TTA)_3$ provides compelling evidence that the Eu complex has been successfully deposited onto the surface of the GF.

As a down-conversion phosphor material, the absorption capacity of GF–Phen–$Eu(TTA)_3$ for ultraviolet-visible light plays a crucial role in its fluorescent properties. The ultraviolet-visible diffuse reflection spectra (UV-Vis DRS) of the materials are depicted in Fig. 2. As shown in figure, the GF exhibits the characteristic absorption spectrum of glass materials in response to ultraviolet light. After chemical coupling treatment with Phen, the glass fiber demonstrated enhanced light absorption in the 320–420 nm, albeit with a subtle effect. For europium complexes-loaded glass fibers, a prominent absorption band in the 305–410 nm range is observed for GF–Phen–$Eu(TTA)_3$, attributed to the exceptional absorption capability of TTA. According to this figure, GF–Phen–$Eu(TTA)_3$ demonstrates the highest absorption capacity in the ultraviolet region at approximately 350 nm which closely aligns with the maximum fluorescence excitation wavelength of GF–Phen–$Eu(TTA)_3$ shown in Fig. 3. This result indicates that GF–Phen–$Eu(TTA)_3$ can absorb abundant energy in the ultraviolet range and then

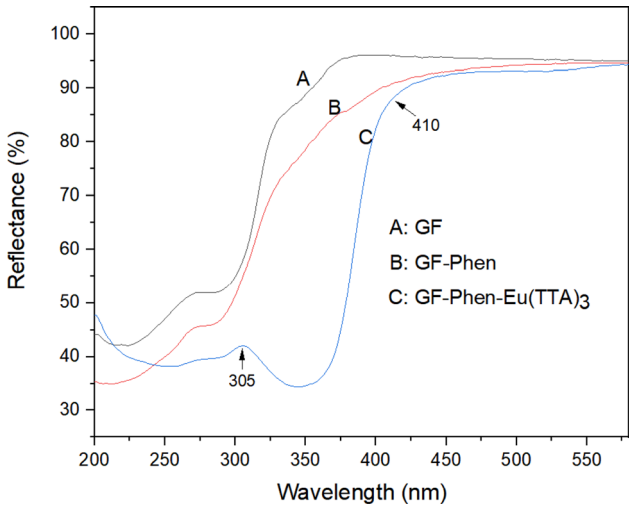


Fig. 2 UV-Vis DRS spectra of GF, GF–Phen and GF–Phen–Eu(TTA)$_3$.

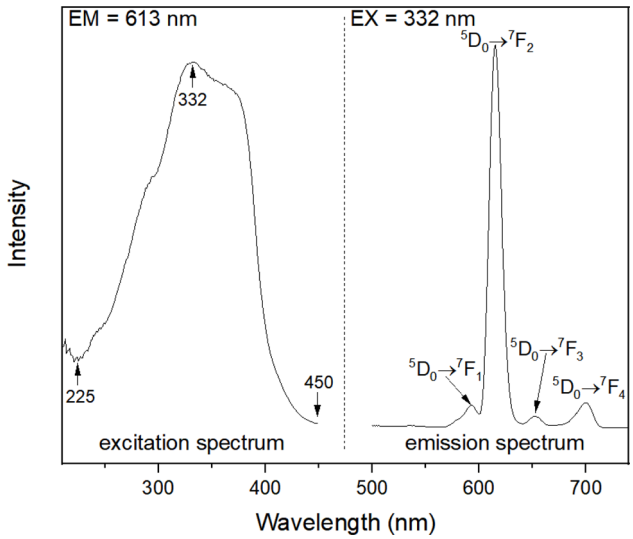


Fig. 3 Fluorescence excitation and emission spectra of GF–Phen–Eu(TTA)$_3$.

transfer it through the "antenna effect" to sensitize the fluorescence emmission properties of the europium(III) ions loaded on glass fiber. Therefore, we can expect that GF–Phen–Eu(TTA)$_3$ will have excellent photoluminescence performance under ultraviolet light, which has been confirmed by their corresponding fluorescence emission spectra (Fig. 3) and their photo under ultraviolet light (Fig. 1).

As previously mentioned, the europium complex-functionalized glass fiber exhibits a vivid red fluorescence when exposed to 365 nm UV light, attributed to the characteristic emission of europium(III) ions. In order to further investigate its fluorescence properties, Fig. 3 illustrates the fluorescence excitation and emission spectra of GF–Phen–Eu(TTA)$_3$. By monitoring the strongest emission peak of europium(III) ions at 613 nm, the fluorescence excitation spectrum can be obtained. The spectrum reveals that the peak of fluorescence excitation spectrum is situated at about 332 nm and exhibits a broad band-like structure. As previously discussed, the excitation band closely aligns with the UV absorption range of the β-diketone (TTA). Based on this, we selected the 332 nm as the excitation wavelength and performed the fluorescence emission measurement of the GF–Phen–Eu(TTA)$_3$. As shown on the right side of Fig. 3, the fluorescence emission spectrum of GF–Phen–Eu(TTA)$_3$ displays the characteristic narrow band emission associated with rare earth elements. There are four distinct emission peaks can be observed from left to right, with their centers located at 592, 613, 652, and 703 nm, which can be aligned to the transitions of europium(III) ions from $^5D_0 \rightarrow {}^7F_1$, $^5D_0 \rightarrow {}^7F_2$, $^5D_0 \rightarrow {}^7F_3$ and $^5D_0 \rightarrow {}^7F_4$ transitions, respectively. It is evident that the overwhelming majority of these emissions lie within the red light spectrum, thereby accounting for its appearance as red under a UV light. It is also evident that the narrowband emission peak corresponding to $^5D_0 \rightarrow {}^7F_2$ transition overwhelmingly dominates, resulting in its exceptionally high purity in the red color. Furthermore, it is widely recognized that the electric dipole transition $^5D_0 \rightarrow {}^7F_2$ of europium(III) ions demonstrates a high sensitivity to local spatial symmetry, while the magnetic dipole transition $^5D_0 \rightarrow {}^7F_1$ of europium(III) ions exhibits relatively low sensitivity to local spatial symmetry. As a result, the ratio ($R$) of emission intensities from the $^5D_0 \rightarrow {}^7F_2$ and $^5D_0 \rightarrow {}^7F_1$ transitions of europium(III) ions (*i.e.* $I(^5D_0 \rightarrow {}^7F_2)/I(^5D_0 \rightarrow {}^7F_1)$) can be seen as a crucial indicator for assessing the radial symmetry around europium(III) ions. Here, the $R$ value of GF–Phen–Eu(TTA)$_3$ is as high as 18.1, indicating that europium(III) ions is situated within an environment of low symmetry, which is in line with the hypothesis that europium(III) ions occupy the coordination center of [Eu(TTA)$_3$Phen] moieties.

The fluorescence decay curve of GF–Phen–Eu(TTA)$_3$ was measured using an excitation wavelength of 332 nm at room temperature (Fig. S2, ESI†). The decay data can be well fitted to a double exponential function, and the decay time was calculated to be about 4.7 μs. Moreover, the $^5D_0$ quantum efficiency of the GF–Phen–Eu(TTA)$_3$ was estimated based on the emission spectra and lifetime ($\tau$), in accordance with the Judd–Ofelt theory (further details are listed in ESI†). The fluorescent quantum efficiency of GF–Phen–Eu(TTA)$_3$ was calculated to be about 0.5%. The relatively low value may be attributed to the limited capacity of the rapid assembly method to accommodate a substantial quantity of europium complex on the glass fiber, thereby resulting in a reduced theoretical quantum efficiency. In short, these optical properties primarily stem from the unique coordination structure of [Eu(TTA)$_3$(Phen)] and its relatively low loading content.[60–62]

As a self-supporting material, one of the most important advantages of glass fiber is that it can be freely cut into a certain shape. In order to further expand the applications of europium complex-loaded glass fiber, the GF–Phen–Eu(TTA)$_3$ was cutted into strips and tested its potential performance in metal ion sensing. The fluorescence response of GF–Phen–Eu(TTA)$_3$ to a range of common metal ions ($Li^+$, $Na^+$, $K^+$, $Ca^{2+}$, $Mg^{2+}$, $Zn^{2+}$, $Cu^{2+}$, $Fe^{3+}$ and $Co^{2+}$) at a concentration of 1 mM was assessed. As shown in Fig. 4, the fluorescence intensity of GF–Phen–

$Eu(TTA)_3$ did not show significant change after immersed in solutions containing $Li^+$, $Na^+$, $K^+$, $Ca^{2+}$ or $Mg^{2+}$; meanwhile, the corresponding strips exhibited negligible color changes when examined under a 365 nm lamp following immersion. However, upon immersion in the solution containing $Zn^{2+}$, $Cu^{2+}$, $Fe^{3+}$ and $Co^{2+}$ ions, the fluorescence intensity of the strips exhibited a significant decrease. This phenomenon is also observable through their fluorescent expression when exposed to a 365 nm light. As shown in the figure, the fluorescence of the strip immersed in solutions containing $Cu^{2+}$, $Fe^{3+}$ and $Co^{2+}$ was significantly quenched. Only the strip immersed in the $Zn^{2+}$ solution exhibited residual weak fluorescence. It is evident that the fluorescence quenching of GF–Phen–$Eu(TTA)_3$ by $Cu^{2+}$, $Fe^{3+}$ and $Co^{2+}$ can be attributed to their strong coordination ability, enabling them to effectively compete with $Eu^{3+}$ for chelating with the Phen moieties. These ions have the capability to displace the europium complex from the surface of glass fiber, consequently leading to the loss of characteristic fluorescence of europium(III) ions for those soaked strips. While for $Zn^{2+}$ ions or other ions that belongs to main group, owing to limited coordination ability, they are unable to effectively displace the europium(III) ions on the paper. Consequently, complete quenching of their fluorescence is unattainable, or their impact on the fluorescence performance of the strip is minimal. These results indicate that the GF–Phen–$Eu(TTA)_3$ exhibits specific selectivity and high sensitivity to some transition metal ions, rendering it a promising metal ion sensor of broad-spectrum.

Regrettably, upon further reduction of the solution concentration, for instance by decreasing the metal ion concentration to 100 μmol, only few transition metal ions, such as $Cu^{2+}$ and $Fe^{3+}$, can effectively quench the fluorescence of the test paper. However, in addition to the cost-effective glass fiber paper and ethanol, the other primary reagents utilized in this study are relatively economical (Table S2, ESI†), and the experimental procedures are straightforward with a high success rate. The production cost for creating the fluorescent test paper described in this study is minimal. Furthermore, the preparation process for this test paper does not necessitate stringent requirements; it can even be conducted in chemistry laboratories at primary and secondary schools. As long as standard safety goggles and gloves are worn during experimentation, it can be safely performed. The resulted GF–Phen–$Eu(TTA)_3$ displays certain stability. A vivid red fluorescence remained detectable under 365 nm UV light even after prolonged storage in a standard ziplock bag within the laboratory for a year. Despite the decrease in fluorescence intensity, it remained suitable for transition metal ion sensing tests. To evaluate the detection capability of the fluorescent paper in real water samples, we collected multiple water samples from a local river and observed that the natural water samples did not quench the fluorescence of our paper. However, introduction of ions such as $Cu^{2+}$ and $Fe^{3+}$ resulted in quenching, indicating potential practical applications for GF–Phen–$Eu(TTA)_3$. Thus, the sensing performance of GF–Phen–$Eu(TTA)_3$ towards transition metal ions demonstrates remarkable environmental stability and resistance to interference.

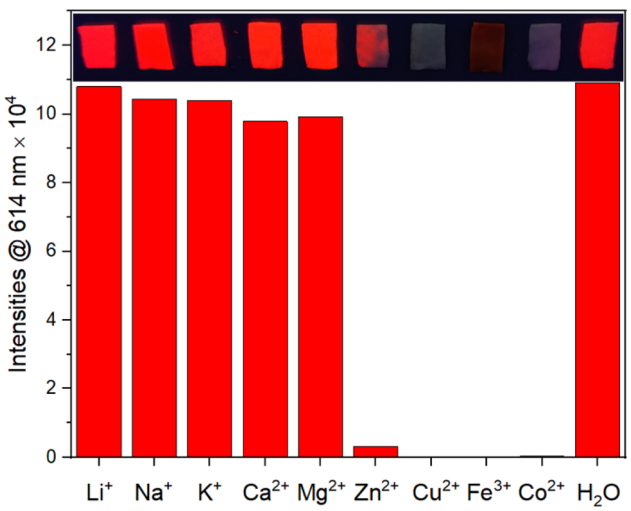


Fig. 4 Photographs of the GF–Phen–$Eu(TTA)_3$ strips under 365 nm UV lamp after treated with different metal ion solutions for 10 min, and comparison of their corresponding fluorescence intensity.

## 4. Conclusions

In this paper, a novel rare earth composite material was synthesized through a simple ultrasonic solvent reaction method using glass fiber as the matrix. The prepared GF–Phen–$Eu(TTA)_3$ have outstanding fluorescent performance and exhibits intense red fluorescence when exposed to 365 nm light. The developed composite material also exhibit good photostability, mechanical properties, suggesting that the GF–Phen–$Eu(TTA)_3$ are a very promising fluorescent materials. Moreover, the inherent self-supporting nature of glass fiber enables GF–Phen–$Eu(TTA)_3$ to be tailored into diverse structures. Here, GF–Phen–$Eu(TTA)_3$ has been fabricated into strip format and observed its specific sensing capability towards some transition metal ions, offering a novel avenue for the development of test strip that can be used for the detecting of transition metal ion.

## Data availability

The data supporting this article have been included as part of the ESI.†

## Conflicts of interest

The authors declare that they have no known competing financial interests or personal relationships that could have appeared to influence the work reported in this paper.

## Acknowledgements

This work was supported by the Research Project of Fuzhou Medical College of Nanchang University (FYKJ202303) and the Science and Technology Research Project of Jiangxi Provincial Department of Education (GJJ218108).

## References


1 M. Gaft, L. Nagli, I. Gornushkin and Y. Raichlin, Review on recent advances in analytical applications of molecular emission and modelling, *Spectrochim. Acta, Part B*, 2020, **173**, 105989.

2 M. J. Weber, *Handbook on the Physics and Chemistry of Rare Earths, Chapter 35 Rare Earth Lasers*, Elsevier, 1979, vol. 4, pp. 275–315.

3 L. U. Khan and Z. U. Khan, *Handbook of Materials Characterization: Rare Earth Luminescence: Electronic Spectroscopy and Applications*, Springer International Publishing, 2018, pp. 345–404.

4 C. R. Ronda, T. Jüstel and H. Nikol, Rare earth phosphors: fundamentals and applications, *J. Alloys Compd.*, 1998, **275–277**, 669–676.

5 N. S. Satpute and S. J. Dhoble, *Energy Materials: Chapter 14 – Role of Rare-Earth Ions for Energy-Saving LED Lighting Devices*, Elsevier, 2021, pp. 407–444.

6 S. B. Li, L. Zhou and H. J. Zhang, Investigation progresses of rare earth complexes as emitters or sensitizers in organic light-emitting diodes, *Light: Sci. Appl.*, 2022, **11**(1), 177.

7 J. Ballato, J. S. Lewis and P. Holloway, Display applications of rare-earth-doped materials, *MRS Bull.*, 1999, **24**(9), 51–56.

8 D. Paderni, L. Giorgi, V. Fusi, M. Formica, G. Ambrosi and M. Micheloni, Chemical sensors for rare earth metal ions, *Coord. Chem. Rev.*, 2021, **429**, 213639.

9 X. Shen and B. Yan, Photoactive rare earth complexes for fluorescence tuning and sensing cations (fe3+) and anions (cr2o72−), *RSC Adv.*, 2015, **5**(9), 6752–6757.

10 D. N. Zhang, Y. Zhou, J. Cuan and N. Gan, A lanthanide functionalized mof hybrid for ratiometric luminescence detection of an anthrax biomarker, *CrystEngComm*, 2018, **20**(9), 1264–1270.

11 C. Bouzigues, T. Gacoin and A. Alexandrou, Biological applications of rare-earth based nanoparticles, *ACS Nano*, 2011, **5**(11), 8488–8505.

12 Y. Li, C. Chen, F. F. Liu and J. L. Liu, Engineered lanthanide-doped upconversion nanoparticles for biosensing and bioimaging application, *Microchim. Acta*, 2022, **189**(3), 109.

13 J. H. S. K. Monteiro, Recent advances in luminescence imaging of biological systems using lanthanide(III) luminescent complexes, *Molecules*, 2020, **25**(9), 2089.

14 J. Cuan, H. Zhou, X. F. Huang, X. H. Cong and Y. Zhou, Hydro-photo-thermo-responsive multicolor luminescence switching of a ternary mof hybrid for advanced information anticounterfeiting, *Small*, 2024, **20**(21), 2305624.

15 C. Y. Zhang, Q. X. Yin, S. K. Ge, J. X. Qi, Q. Y. Han, W. Gao, Y. K. Wang, M. D. Zhang and J. Dong, Optical anti-counterfeiting and information storage based on rare-earth-doped luminescent materials, *Mater. Res. Bull.*, 2024, **176**, 112801.

16 S. Torres-García, C. Hernández-Álvarez, M. Medina-Alayón, P. Acosta-Mora, A. C. Yanes, J. Del-Castillo, A. Menéndez-Velázquez and J. Méndez-Ramos, Tailoring luminescent patterns with rare-earth photonic materials for anti-counterfeiting applications: a lightkey, *Ceram. Int.*, 2023, **49**(14, Part B), 24390–24394.

17 A. Meijerink and R. T. Wegh, Spin-allowed and spin-forbidden $4f^n \leftrightarrow 4f^{n-1}5d$ transitions for heavy lanthanides in fluoride hosts, *Phys. Rev. B: Condens. Matter Mater. Phys.*, 1999, **60**(15), 10820–10830.

18 M. Hatanaka and S. Yabushita, Theoretical study on the f−f transition intensities of lanthanide trihalide systems, *J. Phys. Chem. A*, 2009, **113**(45), 12615–12625.

19 J. Feng and H. J. Zhang, Hybrid materials based on lanthanide organic complexes: a review, *Chem. Soc. Rev.*, 2013, **42**(1), 387–410.

20 K. Binnemans, Lanthanide-based luminescent hybrid materials, *Chem. Rev.*, 2009, **109**(9), 4283–4374.

21 B. Yan, *Photofunctional Rare Earth Hybrid Materials: Rare Earth, Rare Earth Luminescence, Luminescent Rare Earth Compounds, and Photofunctional Rare Earth Hybrid Materials*, Springer, Singapore, 2017, pp. 3–21.

22 Z. M. Wang, L. J. van de Burgt and G. R. Choppin, Spectroscopic study of lanthanide(iii) complexes with carboxylic acids, *Inorg. Chim. Acta*, 1999, **293**(2), 167–177.

23 Y. A. Belousov, A. A. Drozdov, I. V. Taydakov, F. Marchetti, R. Pettinari and C. Pettinari, Lanthanide azolecarboxylate compounds: structure, luminescent properties and applications, *Coord. Chem. Rev.*, 2021, **445**, 214084.

24 X. X. Wang, Y. F. Hao, J. Du, Y. Y. Ma, J. J. Zhao, N. Ren and J. J. Zhang, A series of lanthanide complexes with different aromatic carboxylic acid ligands: synthesis, supramolecular structure, thermal properties and luminescence behaviors, *J. Saudi Chem. Soc.*, 2023, **27**(6), 101763.

25 H. F. Li, P. F. Yan, P. Chen, Y. Wang, H. Xu and G. M. Li, Highly luminescent bis-diketone lanthanide complexes with triple-stranded dinuclear structure, *Dalton Trans.*, 2012, **41**(3), 900–907.

26 A. Dalal, K. Nehra, A. Hooda, D. Singh, P. Kumar, S. Kumar, R. S. Malik and B. Rathi, Luminous lanthanide diketonates: review on synthesis and optoelectronic characterizations, *Inorg. Chim. Acta*, 2023, **550**, 121406.

27 K. Nehra, A. Dalal, A. Hooda, S. Bhagwan, R. K. Saini, B. Mari, S. Kumar and D. Singh, Lanthanides β-diketonate complexes as energy-efficient emissive materials: a review, *J. Mol. Struct.*, 2022, **1249**, 131531.

28 L. N. Zheng, F. H. Wei, H. M. Hu, C. Bai, X. L. Yang, X. F. Wang and G. L. Xue, Lanthanide coordination polymers constructed from the asymmetrical n-heterocyclic rigid carboxylate: synthesis, crystal structures, luminescence properties and magnetic properties, *Polyhedron*, 2019, **161**, 47–55.

29 N. Du, X. Gao, J. Song, Z. N. Wang, Y. H. Xing, F. Y. Bai and Z. Shi, Optical detection of small biomolecule thiamines at a micromolar level by highly luminescent lanthanide complexes with tridentate n-heterocyclic ligands, *RSC Adv.*, 2016, **6**(75), 71012–71024.

30 L. X. You, S. J. Wang, G. Xiong, F. Ding, K. W. Meert, D. Poelman, P. F. Smet, B. Y. Ren, Y. W. Tian and

Y. G. Sun, Synthesis, structure and properties of 2d lanthanide coordination polymers based on n-heterocyclic arylpolycarboxylate ligands, *Dalton Trans.*, 2014, **43**(46), 17385–17394.

31 R. Tan, H. Zhu, C. Cao and O. Chen, Multi-component superstructures self-assembled from nanocrystal building blocks, *Nanoscale*, 2016, **8**(19), 9944–9961.

32 B. Yan, *Photofunctional Rare Earth Hybrid Materials: Photofunctional Rare Earth Hybrid Materials Based on Multicomponent Assembly*, Springer, Singapore, 2017, pp. 167–196.

33 Q. P. Li and B. Yan, Multi-component assembly of luminescent rare earth hybrid materials, *J. Rare Earths*, 2019, **37**(2), 113–123.

34 B. Yan, Recent progress in photofunctional lanthanide hybrid materials, *RSC Adv.*, 2012, **2**(25), 9304–9324.

35 A. K. Singh, Multifunctionality of lanthanide-based luminescent hybrid materials, *Coord. Chem. Rev.*, 2022, **455**, 214365.

36 P. Li and H. R. Li, Recent progress in the lanthanide-complexes based luminescent hybrid materials, *Coord. Chem. Rev.*, 2021, **441**, 213988.

37 A. M. Kaczmarek and P. Van Der Voort, Light-emitting lanthanide periodic mesoporous organosilica (pmo) hybrid materials, *Materials*, 2020, **13**(3), 566.

38 L. Trupp, M. C. Marchi and B. C. Barja, Lanthanide–based luminescent hybrid silica materials prepared by sol-gel methodologies: a review, *J. Sol-Gel Sci. Technol.*, 2022, **102**(1), 63–85.

39 Q. Zhang, W. Y. Ge, X. M. Zhang, Y. Tian and Z. Yin, Silicon-based nanoparticles grafted lanthanide coordination polymer phosphor: facile synthesis, formation process and white light-emitting diodes, *J. Alloys Compd.*, 2023, **967**, 171811.

40 M. Z. Zhang, X. Y. Zhai, M. Z. Sun, T. F. Ma, Y. K. Huang, B. L. Huang, Y. P. Du and C. H. Yan, When rare earth meets carbon nanodots: mechanisms, applications and outlook, *Chem. Soc. Rev.*, 2020, **49**(24), 9220–9248.

41 M. Fang, A. N. C. Neto, L. Fu, R. A. S. Ferreira, V. DeZeaBermudez and L. D. Carlos, A hybrid materials approach for fabricating efficient wleds based on di-ureasils doped with carbon dots and a europium complex, *Adv. Mater. Technol.*, 2022, **7**(3), 2100727.

42 J. Z. Huo, X. S. Li, J. D. An, L. X. Zhang, Y. Li, G. X. Du, X. X. Wu, Y. Y. Liu and B. Ding, Photo-luminescent chiral carbon-dot@eu(d-cam) nanocomposites for selectively luminescence sensing of l-phenylalanine, *J. Mol. Struct.*, 2020, **1201**, 127214.

43 J. Xiao, G. J. Fu, H. X. Liu and S. Ouyang, Effect of al2o3 on the structure and photoluminescence properties of sol-gel glass doped with rare earth organic complex, *Chin. J. Chem.*, 2005, **23**(6), 685–688.

44 M. L. Melgoza-Ramírez and R. Ramírez-Bon, Microstructural comparison between pmma-sio2 and pmma-tio2 hybrid systems using eu3+ as ion-probe luminescence, *J. Non-Cryst. Solids*, 2020, **544**, 120167.

45 B. Yan, H. C. Wu, P. T. Ma, J. Y. Niu and J. P. Wang, Recent advances in rare earth co-doped luminescent tungsten oxygen complexes, *Inorg. Chem. Front.*, 2021, **8**(18), 4158–4176.

46 Y. W. Wu, H. X. Hao, Q. Y. Wu, Z. H. Gao and H. D. Xie, Preparation and luminescent properties of the novel polymer-rare earth complexes composed of poly(ethylene-co-acrylic acid) and europium ions, *Opt. Mater.*, 2018, **80**, 65–70.

47 W. C. Zhao, H. F. Shao, G. Yu, Y. J. Hou and S. H. Wang, The coordination and luminescence of the eu(III) complexes with the polymers (pmma, pvp), *Polymers*, 2018, **10**(5), 508.

48 Z. F. Wang, W. W. Ye, X. R. Luo and Z. G. Wang, Fabrication of superhydrophobic and luminescent rare earth/polymer complex films, *Sci. Rep.*, 2016, **6**(1), 24682.

49 Y. G. Wang, P. Li, S. F. Wang and H. R. Li, Recent progress in luminescent materials based on lanthanide complexes intercalated synthetic clays, *J. Rare Earths*, 2019, **37**(5), 451–467.

50 L. Guo, X. L. Tian, C. Y. Zhu, S. Hussain, J. F. Han and H. R. Li, A dual-emission fluorescent ratiometric probe based on bimetallic lanthanide complex interacted in nanoclay for monitoring of food spoilage, *Sens. Actuators, B*, 2022, **366**, 131992.

51 K. S. Ambili and J. Thomas, Synthesis of hybrid materials by immobilizing para-aminobenzoic acid complexes of eu3+ and tb3+ in zeolite y and their luminescent properties, *J. Porous Mater.*, 2020, **27**(3), 755–764.

52 J. Q. Liu, Z. D. Luo, Y. Pan, A. Kumar Singh, M. Trivedi and A. Kumar, Recent developments in luminescent coordination polymers: designing strategies, sensing application and theoretical evidences, *Coord. Chem. Rev.*, 2020, **406**, 213145.

53 C. A. T. Laia and A. Ruivo, *Fluorescence in Industry: Photoluminescent Glasses and Their Applications*, Springer International Publishing, 2019, pp. 365–388.

54 X. F. Guo, K. Q. Zhang, H. W. Zhang and M. Q. Ge, Working conditions on the afterglow characteristics of rare-earth luminous fibers, *Fibers Polym.*, 2018, **19**(3), 531–537.

55 G. Santos, M. R. Cavallari, F. J. Fonseca and L. Pereira, Oxygen plasma surface treatment onto ito surface for oleds based on europium complex, *J. Integr. Circuits Syst.*, 2015, **10**(1), 7–12.

56 M. C. Shang, J. J. Zhang, Z. Zhou, F. Shi and Z. Q. Wang, Fabrication and luminescence properties of rare earth complex grafted carbon fiber, *Compos. Commun.*, 2023, **37**, 101471.

57 Y. J. Tong, L. D. Yu, Y. J. Huang, Q. Fu, N. Li, S. Peng, S. Ouyang, Y. X. Ye, J. Q. Xu, F. Zhu, J. Pawliszyn and G. F. Ouyang, Polymer ligand-sensitized lanthanide metal–organic frameworks for an on-site analysis of a radionuclide, *Anal. Chem.*, 2021, **93**(26), 9226–9234.

58 J. Singh, M. Kumar, S. Kumar and S. K. Mohapatra, Properties of glass-fiber hybrid composites: a review, *Polym.-Plast. Technol. Eng.*, 2017, **56**(5), 455–469.

59 S. Maiti, M. R. Islam, M. A. Uddin, S. Afroj, S. J. Eichhorn and N. Karim, Sustainable fiber-reinforced composites: a review, *Adv. Sustainable Syst.*, 2022, **6**(11), 2200258.

60 R. A. N. Silva, J. D. C. Menezes, G. C. Marineli, M. A. Cebim, M. R. Davolos, S. A. M. Lima and A. M. Pires, [$Eu(TTA)_3$(phen-derived)] complexes: theoretical and empirical approaches enlightening their photophysical behavior, *J. Lumin.*, 2024, **270**, 120563.

61 Y. K. Hong, H. T. Kim, Y. Park, W. Jeong, M. Kim, E. Hwang, Y. J. Hwang, M. H. Lee and D. H. Ha, Design of eu(tta)3phen-incorporated $SiO_2$-coated transition metal oxide nanoparticles for efficient luminescence and magnetic performance, *Nanoscale*, 2023, **15**(9), 4604–4611.

62 Z. H. Wang, X. L. Hu, Y. Q. Yang, W. Wang, Y. Wang, X. Z. Gong, C. Y. Geng and J. G. Tang, Synthesis of mesoporous and hollow $SiO_2$@ $Eu(TTA)_3$phen with enhanced fluorescence properties, *Materials*, 2023, **16**(13), 4501.